JCI The Journal of Clinical Investigation

Antibody-based targeting of FGFR3 in bladder carcinoma and t(4;14)-positive multiple myeloma in mice

Jing Qing, Xiangnan Du, Yongmei Chen, Pamela Chan, Hao Li, Ping Wu, Scot Marsters, Scott Stawicki, Janet Tien, Klara Totpal, Sarajane Ross, Susanna Stinson, David Dornan, Dorothy French, Qian-Rena Wang, Jean-Philippe Stephan, Yan Wu, Christian Wiesmann, Avi Ashkenazi

Research Article

Overexpression of FGF receptor 3 (FGFR3) is implicated in the development of t(4;14)-positive multiple myeloma. While FGFR3 is frequently overexpressed and/or activated through mutations in bladder cancer, the functional importance of FGFR3 and its potential as a specific therapeutic target in this disease have not been elucidated in vivo. Here we report that inducible knockdown of FGFR3 in human bladder carcinoma cells arrested cell-cycle progression in culture and markedly attenuated tumor progression in xenografted mice. Further, we developed a unique antibody (R3Mab) that inhibited not only WT FGFR3, but also various mutants of the receptor, including disulfide-linked cysteine mutants. Biochemical analysis and 2.1-Å resolution crystallography revealed that R3Mab bound to a specific FGFR3 epitope that simultaneously blocked ligand binding, prevented receptor dimerization, and induced substantial conformational changes in the receptor. R3Mab exerted potent antitumor activity against bladder carcinoma and t(4;14)-positive multiple myeloma xenografts in mice by antagonizing FGFR3 signaling and eliciting antibody-dependent cell-mediated cytotoxicity (ADCC). These studies provide in vivo evidence demonstrating an oncogenic role of FGFR3 in bladder cancer and support antibody-based targeting of FGFR3 in hematologic and epithelial cancers driven by WT or mutant FGFR3.

Find the latest version:

Antibody-based targeting of FGFR3 in bladder carcinoma and t(4;14)-positive multiple myeloma in mice

Jing Qing,[1] Xiangnan Du,[1] Yongmei Chen,[2] Pamela Chan,[3] Hao Li,[4] Ping Wu,[5]
Scot Marsters,[1] Scott Stawicki,[2] Janet Tien,[4] Klara Totpal,[4] Sarajane Ross,[4]
Susanna Stinson,[6] David Dornan,[6] Dorothy French,[7] Qian-Rena Wang,[1]
Jean-Philippe Stephan,[3] Yan Wu,[2] Christian Wiesmann,[5] and Avi Ashkenazi[1]

[1]Department of Molecular Oncology, [2]Department of Antibody Engineering, [3]Department of Assay Automation and Technology,
[4]Department of Cancer Signaling and Translational Oncology, [5]Department of Protein Engineering,
[6]Department of Oncology Research Diagnostics, and [7]Department of Pathology, Genentech Inc., South San Francisco, California, USA.

Overexpression of FGF receptor 3 (FGFR3) is implicated in the development of t(4;14)-positive multiple myeloma. While FGFR3 is frequently overexpressed and/or activated through mutations in bladder cancer, the functional importance of FGFR3 and its potential as a specific therapeutic target in this disease have not been elucidated in vivo. Here we report that inducible knockdown of FGFR3 in human bladder carcinoma cells arrested cell-cycle progression in culture and markedly attenuated tumor progression in xenografted mice. Further, we developed a unique antibody (R3Mab) that inhibited not only WT FGFR3, but also various mutants of the receptor, including disulfide-linked cysteine mutants. Biochemical analysis and 2.1-Å resolution crystallography revealed that R3Mab bound to a specific FGFR3 epitope that simultaneously blocked ligand binding, prevented receptor dimerization, and induced substantial conformational changes in the receptor. R3Mab exerted potent antitumor activity against bladder carcinoma and t(4;14)-positive multiple myeloma xenografts in mice by antagonizing FGFR3 signaling and eliciting antibody-dependent cell-mediated cytotoxicity (ADCC). These studies provide in vivo evidence demonstrating an oncogenic role of FGFR3 in bladder cancer and support antibody-based targeting of FGFR3 in hematologic and epithelial cancers driven by WT or mutant FGFR3.

Introduction

FGFs and FGF receptors (FGFRs) play critical roles during embryonic development, tissue homeostasis, and metabolism (1–3). In humans, there are 22 FGFs (FGF1–14, FGF16–23) and 4 FGF receptors with tyrosine kinase domains (FGFR1–4). FGFRs consist of an extracellular ligand-binding region, with 2 or 3 immunoglobulin-like domains (IgD1–3), a single-pass transmembrane region, and a cytoplasmic, split tyrosine kinase domain. FGFR1, -2, and -3 each have 2 major alternatively spliced isoforms, designated IIIb and IIIc. These isoforms differ by about 50 amino acids in the second half of IgD3 and have distinct tissue distribution and ligand specificity. In general, the IIIb isoform is found in epithelial cells, whereas IIIc is expressed in mesenchymal cells. Upon binding FGF in concert with heparan sulfate proteoglycans, FGFRs dimerize and become phosphorylated at specific tyrosine residues. This facilitates the recruitment of critical adaptor proteins, such as FGFR substrate 2 α (FRS2α), leading to activation of multiple signaling cascades, including the MAPK and PI3K/Akt pathways (1, 3, 4). Consequently, FGFs and their cognate receptors regulate a broad array of cellular processes, including proliferation, differentiation, migration, and survival, in a context-dependent manner.

Aberrantly activated FGFRs have been implicated in specific human malignancies (1, 5). In particular, the t(4;14)(p16.3;q32) chromosomal translocation occurs in about 15%–20% of multiple myeloma patients, leading to overexpression of FGFR3, and correlates with shorter overall survival (6–9). FGFR3 is also implicated in conferring chemoresistance to myeloma cell lines in culture (10), consistent with the poor clinical response of t(4;14)-positive patients to conventional chemotherapy (8). Overexpression of mutationally activated FGFR3 is sufficient to induce oncogenic transformation in hematopoietic cells and fibroblasts (11–15), transgenic mouse models (16), and murine bone marrow transplantation models (16, 17). Accordingly, FGFR3 has been proposed as a potential therapeutic target in multiple myeloma. Indeed, several small-molecule inhibitors targeting FGFRs, although not selective for FGFR3 and having cross-inhibitory activity toward certain other kinases, have demonstrated cytotoxicity against FGFR3-positive myeloma cells in culture and in mouse models (18–22).

FGFR3 overexpression has also been documented in a high fraction of bladder cancers (23, 24). Furthermore, somatic activating mutations in FGFR3 have been identified in 60%–70% of papillary and 16%–20% of muscle-invasive bladder carcinomas (24, 25). In cell culture experiments, RNA interference (11, 26) or an anti-FGFR3 single-chain Fv antibody fragment inhibited bladder cancer cell proliferation (27). A recent study demonstrated that an anti-FGFR3 antibody–toxin conjugate attenuates xenograft growth of a bladder cancer cell line through FGFR3-mediated toxin delivery into tumors (28). However, it remains unclear whether FGFR3 signaling is indeed an oncogenic driver

---

of in vivo growth of bladder tumors. Moreover, the therapeutic potential for targeting FGFR3 in bladder cancer has not been defined on the basis of in vivo models.

To assess the role of FGFR3 in bladder carcinogenesis, we used inducible shRNA to reduce FGFR3 expression. Knockdown of FGFR3 in bladder cancer cells caused G_1 cell-cycle arrest in vitro and significantly attenuated tumor growth in vivo. Further, we generated a unique function-blocking monoclonal antibody specific to FGFR3 (R3Mab). Remarkably, R3Mab was capable of inhibiting both WT and various cancer-associated mutant forms of FGFR3, including disulfide-linked cysteine mutants. X-ray crystallographic analysis revealed that R3Mab recognizes a unique epitope on FGFR3, which enables it simultaneously to prevent FGF binding and receptor dimerization, as well as to induce significant conformational changes in FGFR3. R3Mab inhibited growth of bladder cancer xenografts expressing WT or mutant FGFR3 by blocking receptor signaling. Furthermore, it inhibited growth of t(4;14)-positive multiple myeloma xenografts via antibody-dependent cell-mediated cytotoxicity (ADCC). These studies indicate that FGFR3 plays an important role in bladder cancer growth and provide a strong rationale for antibody-based therapeutic targeting of FGFR3 in bladder cancer and t(4;14)-positive multiple myeloma.

Results

Inducible shRNA knockdown of FGFR3 attenuates bladder cancer growth in vivo. As a prelude to assessing the importance of FGFR3 for bladder tumor growth in vivo, we examined the effect of FGFR3 knockdown in vitro. Several FGFR3 siRNAs effectively downregulated FGFR3 in bladder cancer cell lines expressing either WT (RT112, RT4, SW780) or mutant (UMUC-14, S249C mutation) FGFR3. FGFR3 knockdown in all 4 cell lines markedly suppressed proliferation in culture (Supplemental Figure 1; supplemental material available online with this article; doi:10.1172/JCI38017DS1). Next, we generated stable RT112 cell lines expressing doxycycline-inducible FGFR3 shRNA. Induction of 3 independent FGFR3 shRNAs by doxycycline diminished FGFR3 expression, whereas induction of a control shRNA targeting EGFP had no effect (Figure 1A). In the absence of exogenous FGF, doxycycline treatment reduced [^{3}H]thymidine incorporation by cells expressing different FGFR3 shRNAs, but not control shRNA (Figure 1B), confirming that FGFR3 knockdown inhibits proliferation. Further analysis of exponentially growing RT112 cells revealed that FGFR3 knockdown over a 72-hour treatment with doxycycline markedly and specifically reduced the percentage of cells in the S and G_2 phases of the cell cycle, with a concomitant increase in cells in G_1 phase (Figure 1C). A similar effect was observed with 2 other FGFR3 shRNAs (Supplemental Figure 2A). No significant numbers of cells with a subdiploid DNA content were detected, suggesting no change in apoptosis levels. Hence, the inhibitory effect of FGFR3 knockdown on the proliferation of RT112 cells is mainly due to attenuation of cell-cycle progression.

We next evaluated the effect of FGFR3 knockdown on the growth of preestablished RT112 tumor xenografts in mice. FGFR3 knockdown substantially and specifically suppressed tumor growth (Figure 1D, top panels, and Supplemental Figure 2B). Analysis of day 45 tumor samples confirmed effective FGFR3 knockdown upon doxycycline induction of FGFR3 shRNA as compared with control shRNA (Figure 1D, bottom
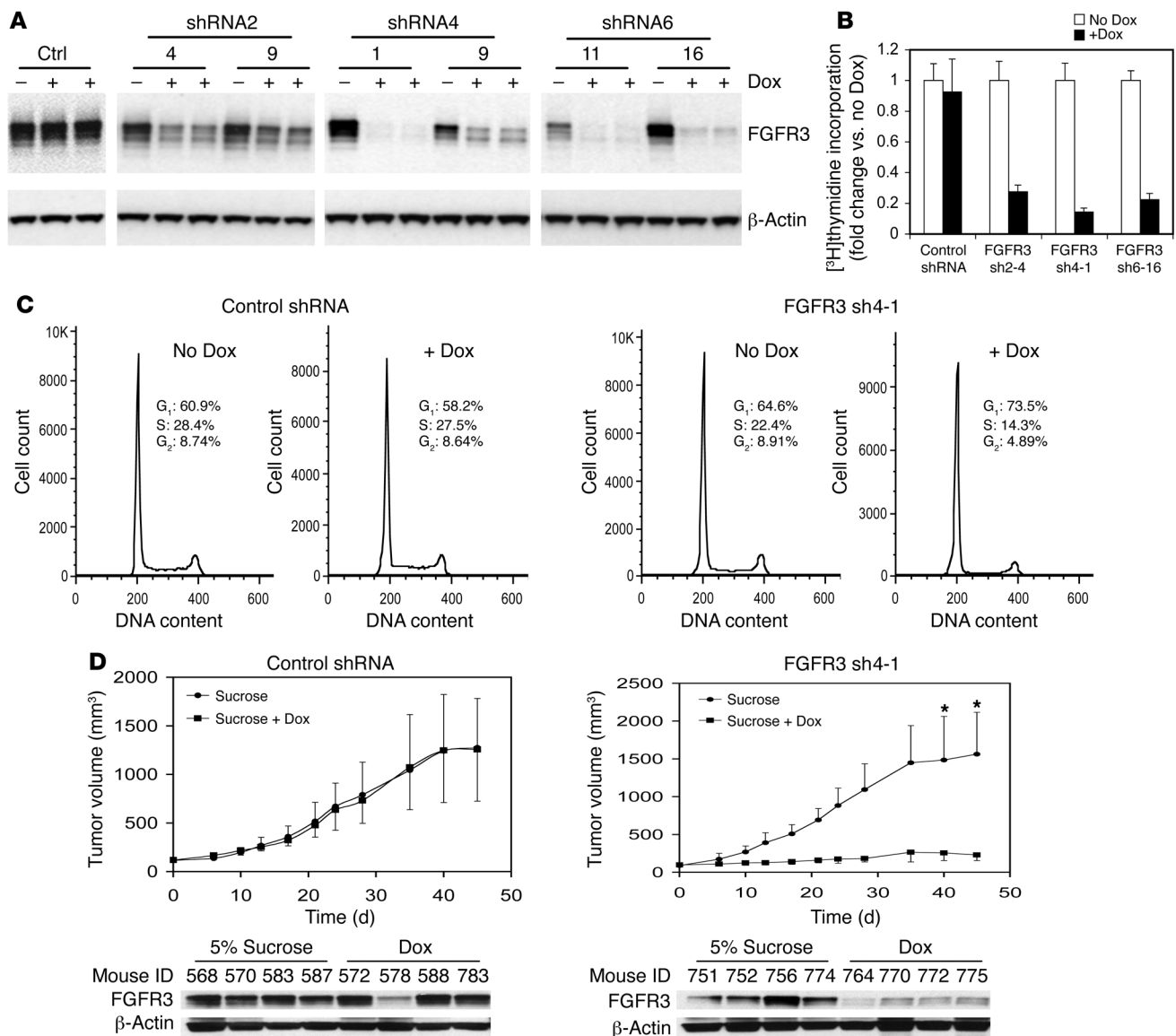
panels). These results demonstrate that FGFR3 is critically important both in vitro and in vivo for the growth of RT112 bladder cancer cells.

Generation of a blocking anti-FGFR3 monoclonal antibody. To examine further the importance of FGFR3 in tumor growth and to explore the potential of this receptor as a therapeutic target, we developed an antagonistic anti-FGFR3 monoclonal antibody (R3Mab) using a phage display approach. We selected this particular antibody based on its ability to block both ligand binding and dimerization by FGFR3 and its unique capacity to inhibit not only WT FGFR3 but also the most prevalent cancer-associated mutants of this receptor (see below). R3Mab targets the extracellular IgD2 and IgD3 domains of FGFR3, which are necessary and sufficient for FGF binding (4). R3Mab bound both the IIIb and IIIc isoforms of human FGFR3 but showed no detectable binding to FGFR1, FGFR2, or FGFR4 (Figure 2A). Surface plasmon resonance analysis indicated that R3Mab had similar apparent affinity to murine, cynomolgus monkey, and human FGFR3-IIIc (data not shown).

We next tested the ability of R3Mab to block FGFR3 binding to FGF1 and FGF9. R3Mab strongly inhibited binding of FGF1 to FGFR3-IIIb and -IIIc, with IC_{50} values of 0.3 nM and 1.7 nM, respectively (Figure 2, B and C). Similarly, R3Mab efficiently blocked FGF9 binding to FGFR3-IIIb and -IIIc, with IC_{50} values of 1.1 nM and 1.3 nM, respectively (Figure 2, D and E).

R3Mab inhibits WT FGFR3 and its most prevalent cancer-associated mutant variants. To examine whether R3Mab inhibits cell proliferation driven by WT or mutant FGFR3, we took advantage of the observation that ectopic FGFR3 expression in murine pro-B Ba/F3 cells confers IL-3–independent, FGF1-dependent proliferation and survival (29). In the absence of FGF1 and IL-3, Ba/F3 cells stably expressing WT FGFR3 were not viable, while FGF1 greatly enhanced their proliferation (Figure 3A). R3Mab specifically blocked FGF1-stimulated Ba/F3-FGFR3 cell proliferation in a dose-dependent manner (Figure 3A). We next evaluated the impact of R3Mab on FGFR3 signaling in these cells. FGF1 induced phosphorylation and activation of FGFR3 and concomitant activation of p44/42 MAPK, while R3Mab effectively suppressed the activation of both molecules (Figure 3B).
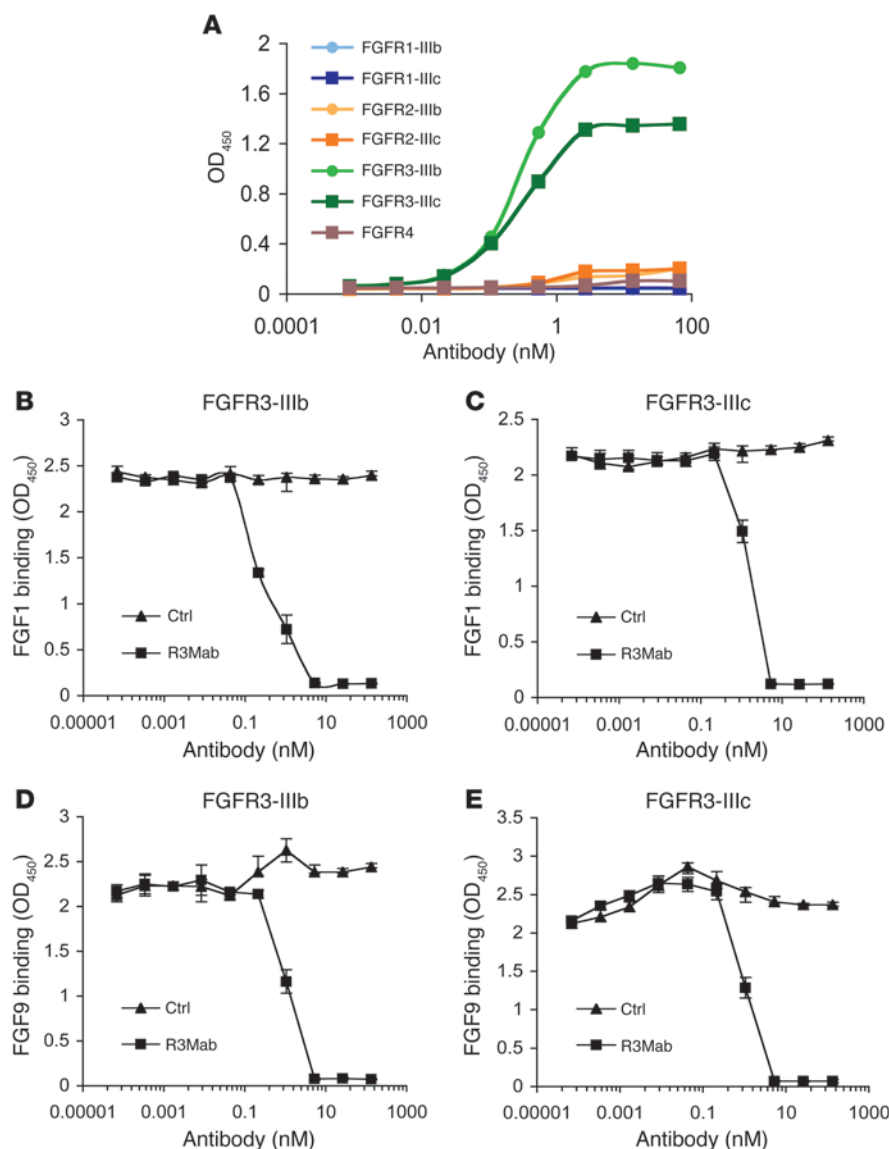
In bladder cancer, somatic activating mutations in FGFR3 cluster within the linker region between IgD2 and IgD3, the extracellular juxtamembrane domain, or the kinase domain (Figure 3C). The extracellular missense substitutions most often give rise to an unpaired cysteine, leading to ligand-independent dimerization of FGFR3. These mutations cause markedly different levels of constitutive FGFR3 activation, possibly owing to a differential impact on the orientation of the cytoplasmic kinase domain (30, 31). The most frequent mutations are S249C, Y375C, R248C, G372C, and K652E, which together account for 98% of all FGFR3 mutations in bladder cancer (32). We reasoned that an optimal therapeutic agent should block not only the WT FGFR3 protein, which is overexpressed in certain cancers, but also the most prevalent tumor-associated FGFR3 mutants. To assess R3Mab further, we generated Ba/F3 cell lines stably expressing each of the 5 most common FGFR3 mutant variants. All mutants were expressed at similar levels at the cell surface, and the cysteine mutants dimerized spontaneously without ligand (data not shown). Cell lines expressing different cysteine mutants exhibited a variable growth response to FGF1, consistent with earlier findings (30, 31). As previously reported (33), cells expressing FGFR3^{R248C} displayed con-

Figure 1

FGFR3 knockdown in RT112 bladder cancer cells inhibits proliferation and induces G_1 cell-cycle arrest in vitro, and it suppresses tumor growth in vivo. Three different FGFR3 shRNAs were cloned into a Tet-inducible expression vector. RT112 cells stably expressing FGFR3 shRNAs or a control shRNA were established with puromycin selection. (**A**) Representative blots showing FGFR3 expression in selected clones treated with or without doxycycline (Dox; 0, 0.1, and 1 μg/ml, left to right). (**B**) [³H]thymidine incorporation by stable RT112 clones. Selected RT112 stable clones, namely clone 4 for FGFR3 shRNA2 (sh2-4), clone 1 for FGFR3 shRNA4 (sh4-1), and clone 16 for FGFR3 shRNA6 (sh6-16), were cultured with or without 1 μg/ml doxycycline for 3 days prior to 16-hour incubation with [³H]thymidine (1 μCi per well). Counts of incorporated [³H]thymidine (in cpm) were normalized to those from cells without doxycycline induction. Error bars represent SEM. (**C**) DNA fluorescence flow cytometry histograms of RT112 stable cells. RT112 clones expressing control shRNA or FGFR3 shRNA4 were cultured with or without 1 μg/ml doxycycline for 72 hours, and the nuclei were stained with propidium iodide (PI). Similar results were obtained for FGFR3 shRNA2 and -6 (Supplemental Figure 2). (**D**) The growth of RT112 cells expressing control shRNA (*n* = 9 per treatment group) or FGFR3 shRNA4 (*n* = 11 per treatment group) in mice. Mice were given 5% sucrose alone or supplemented with 1 mg/ml doxycycline, and tumor size was measured twice a week. Error bars represent SEM. Similar results were obtained for FGFR3 shRNA2 and -6 (Supplemental Figure 2). *P* < 0.0001. Lower panel: Expression of FGFR3 protein in tumor lysates extracted from control shRNA or FGFR3 shRNA4 stable cell xenograft tissues.

stitutive, ligand-independent proliferation and were not responsive to FGF1 (Figure 3D). Similarly, the most frequent mutation, FGFR3[S249C], conferred ligand-independent proliferation (Figure 3E). Remarkably, R3Mab suppressed constitutive proliferation driven by either mutant (Figure 3, D and E). Cells expressing the juxtamembrane domain mutations FGFR3[G372C] (Figure 3F)

or FGFR3[Y375C] (Figure 3G) required FGF1 for proliferation, and their growth was completely blocked by R3Mab. Cells expressing FGFR3[K652E] showed weak ligand-independent proliferation and significant growth in response to FGF1 (33). R3Mab did not affect the weak basal activity of FGFR3[K652E] (data not shown) but nearly abolished ligand-induced proliferation mediated by this mutant

Figure 2
R3Mab blocks FGF-FGFR3 interaction. (**A**) Selective binding of human FGFR3 by R3Mab. Human FGFR1–4 Fc chimeric proteins were immobilized and incubated with increasing amounts of R3Mab. Specific binding was detected using an anti-human Fab antibody. (**B** and **C**) Blocking of FGF1 binding to human FGFR3-IIIb (**B**) or -IIIc (**C**) by R3Mab. Specific binding was detected by using a biotinylated FGF1-specific polyclonal antibody. (**D** and **E**) Blocking of FGF9 binding to human FGFR3-IIIb (**D**) or -IIIc (**E**) by R3Mab. Specific binding was detected by using a biotinylated FGF9-specific polyclonal antibody. Error bars represent SEM and are sometimes smaller than symbols.

(Figure 3H). In a separate effort, we generated and characterized multiple mouse anti–human FGFR3 hybridoma antibodies. None of the hybridoma antibodies could inhibit all the cancer-linked FGFR3 mutants we tested (Supplemental Figure 3), nor did they share overlapping epitopes with R3Mab (data not shown). Hence, R3Mab has a unique capacity to inhibit both WT and prevalent cancer-associated mutants of FGFR3.

Structural basis for the interaction of R3Mab with FGFR3. To gain insight into R3Mab's mode of interaction with FGFR3, we synthesized a panel of 13 overlapping peptides spanning the FGFR3 IgD2 and -D3 regions and tested their binding to R3Mab. Pep-

tides 3 (residues 164–178) and 11 (residues 269–283) showed specific binding to R3Mab, with peptide 3 having a stronger interaction (Figure 4A), indicating that the corresponding regions on FGFR3 are critical for recognition by R3Mab. Previous crystallographic studies of FGFR1 in complex with FGF2 identified critical receptor residues engaged in direct binding to FGF and heparin, as well as in receptor dimerization (34). Alignment of FGFR3 peptides 3 and 11 with the functionally important sites in FGFR1 revealed that these peptides encompass corresponding FGFR1 residues essential for direct FGF2 binding, receptor dimerization, as well as interaction with heparin (Figure 4B). These data indicate that the epitope of R3Mab on FGFR3 overlaps with receptor residues engaged in ligand association and receptor-receptor interaction.

We next crystallized the complex between the Fab fragment of R3Mab and the extracellular IgD2–D3 region of human FGFR3-IIIb and determined the X-ray structure at 2.1-Å resolution (Figure 4, C and D, and Supplemental Table 1). In this complex, approximately 1,400 Å² and 1,500 Å² of solvent-accessible surface areas were buried on FGFR3 and the Fab, respectively. About 80% of the buried interface involved IgD2, while the remainder entailed the linker and IgD3 regions. On the Fab side of the complex, about 40% of the buried interface involved complementarity-determining region H3 (CDR-H3); 20%, CDR-H2; 20%, CDR-L2; and minor contributions were from other CDRs and framework residues. Notably, aa from CDR-H3 formed 2 β-strands, which extended the β-sheet of IgD2 (Figure 4D). The Fab interacted with aa that constituted the FGF binding site of FGFR3 as well as residues that formed the receptor dimerization interface, as previously identified in various dimeric FGF-FGFR complexes (e.g., PDB code 1CVS [ref. 34]; and Figure 4C,

areas in violet and orange). The interaction interfaces identified by crystallography were fully consistent with the peptide-based data (Supplemental Figure 4, A and B). Together, these results reveal how R3Mab inhibits ligand binding and further suggest that binding of R3Mab to FGFR3 may prevent receptor dimerization.

We compared the R3Mab-FGFR3 structure with a previously published structure of FGFR3-IIIc in complex with FGF1 (4, 35) (Figure 4E). Superposition of the antibody-receptor and ligand-receptor complexes revealed that there are no major conformational differences within the individual receptor domains, except in the region that distinguishes FGFR3-IIIc from FGFR3-IIIb; however,
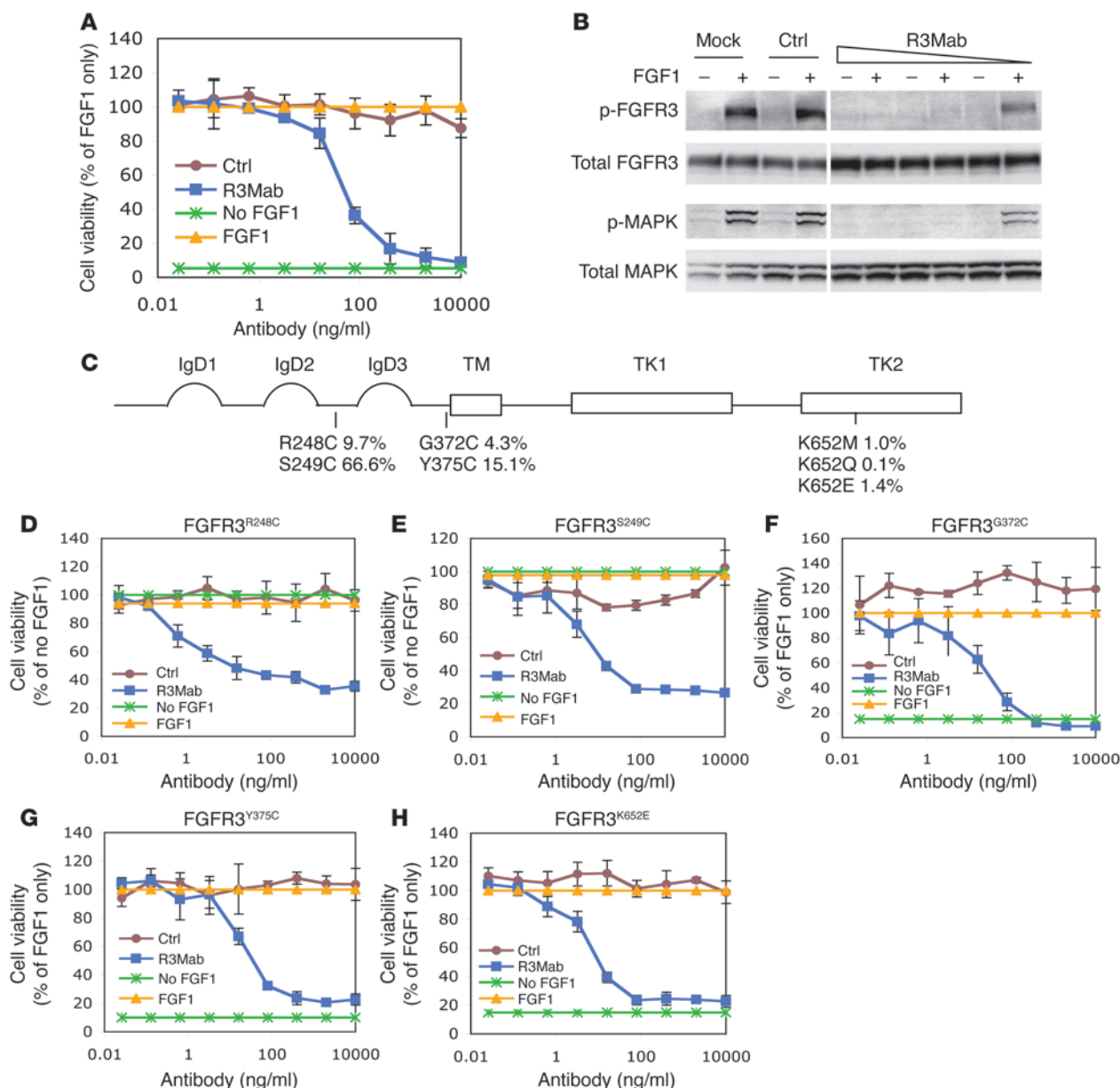
Figure 3
R3Mab inhibits Ba/F3 cell proliferation driven by WT and mutated FGFR3. (**A**) Inhibitory effect of R3Mab on the viability of Ba/F3 cells expressing WT human FGFR3-IIIb. Cells were cultured in medium without FGF1 (No FGF1), in the presence of 10 ng/ml FGF1 plus 10 μg/ml heparin alone (FGF1), or in combination with a control antibody (Ctrl) or R3Mab. Cell viability was assessed with CellTiter-Glo (Promega) after 72-hour incubation with antibodies. (**B**) Inhibition of FGFR3 and MAPK phosphorylation by R3Mab in Ba/F3–FGFR3-IIIb[WT] stable cells. Cells were treated with 15 ng/ml FGF1 and 10 μg/ml heparin (+) or heparin alone (–) for 10 minutes, following preincubation with a control Ab, decreasing amounts of R3Mab (1, 0.2, and 0.04 μg/ml) in PBS, or PBS alone (Mock) for 3 hours. Lysates were immunoblotted to assess phosphorylation of FGFR3 and p44/42 MAPK with antibodies against pFGFR[Y653/654] and p-MAPK[Thr202/Tyr204], respectively. (**C**) Schematic representation of FGFR3 mutation hot spots and frequency in bladder cancer based on published data (32). TM, transmembrane domain; TK1 and TK2, tyrosine kinase domains 1 and 2. (**D–H**) Inhibitory effect of R3Mab on the viability of Ba/F3 cells expressing cancer-associated FGFR3 mutants. G372C is derived from the IIIc isoform, and the other mutants are derived from the IIIb isoform. Cell viability was assessed after 72-hour incubation with antibodies as described in **A**. Error bars represent SEM.

the orientation of IgD3 relative to IgD2 was drastically different (Figure 4E, white and cyan). Since the relative positions of IgD2 and IgD3 are critical for ligand binding, the alternate conformation adopted by IgD3 upon R3Mab binding may provide an additional mechanism to prevent ligand interaction with FGFR3.

R3Mab inhibits endogenous WT and mutant FGFR3 in bladder cancer cells. To assess whether R3Mab could suppress FGFR3 function in bladder cancer cells, we first examined RT112 and RT4 cells, which express WT FGFR3. R3Mab strongly inhibited [3H]thymidine incorporation by RT112 cells (Figure 5A) and exert-
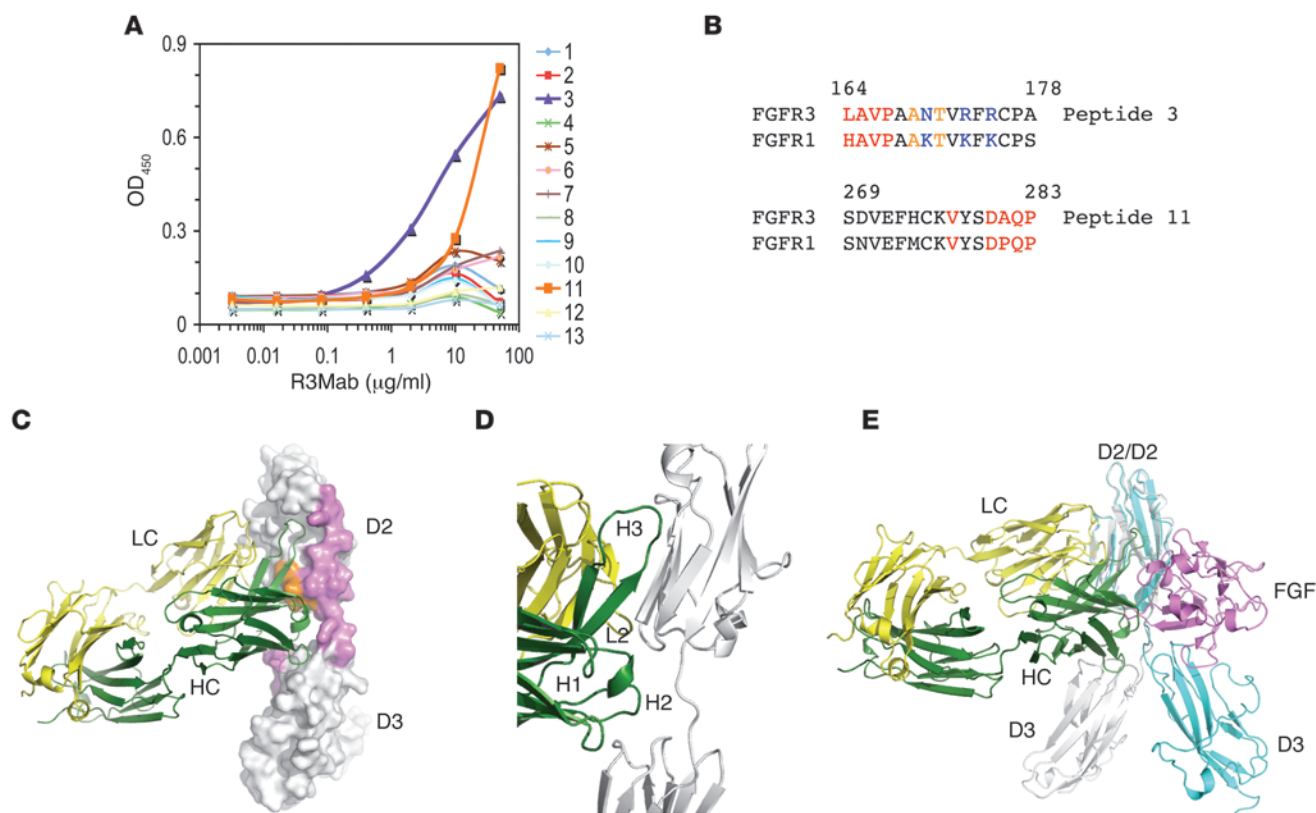
Figure 4
Epitope mapping for R3Mab and crystal structure of the complex between R3Mab Fab fragment and IgD2–D3 of human FGFR3-IIIb. (**A**) Epitope determined by the binding of 13 peptides spanning IgD2–D3 of human FGFR3 to R3Mab. Each biotinylated peptide was captured onto a streptavidin-coated microtiter well and incubated with R3Mab. Specifically bound R3Mab was detected using a goat anti-human IgG antibody. (**B**) Sequence alignment of human FGFR3 peptides 3 and 11 with extracellular segments of human FGFR1. FGFR1 residues engaged in the primary FGF2-FGFR1 interaction, heparin binding, and receptor-receptor association are shown in red, blue, and orange, respectively. Functional assignment of FGFR1 residues is based on the work of Plotnikov et al. (34). (**C**) Structure of R3Mab Fab (shown in ribbon-helix: light chain, yellow; heavy chain, green) in complex with human FGFR3 IgD2–D3 (shown in molecular surface, white). Receptor residues involved in ligand binding and dimerization are colored in violet and orange, respectively, based on the work of Plotnikov et al. (34). (**D**) The close-up of the crystal structure shows that CDR-H3 and -H2 from the Fab constitute the major interaction sites with IgD2 and IgD3 of FGFR3. (**E**) Superposition of the FGFR3-IIIc–FGF1 complex (Protein Data Bank code 1RY7) with the FGFR3-IIIb–Fab complex. FGFR3-IIIc and FGF1 are shown in cyan and violet, respectively. FGFR3-IIIb is shown in white, and the Fab is shown in yellow for light chain, green for heavy chain. IgD2 was used as the anchor for superposition. Note the well-superposed IgD2 from both structures and the new conformation adopted by IgD3 of FGFR3-IIIb when bound by R3Mab.
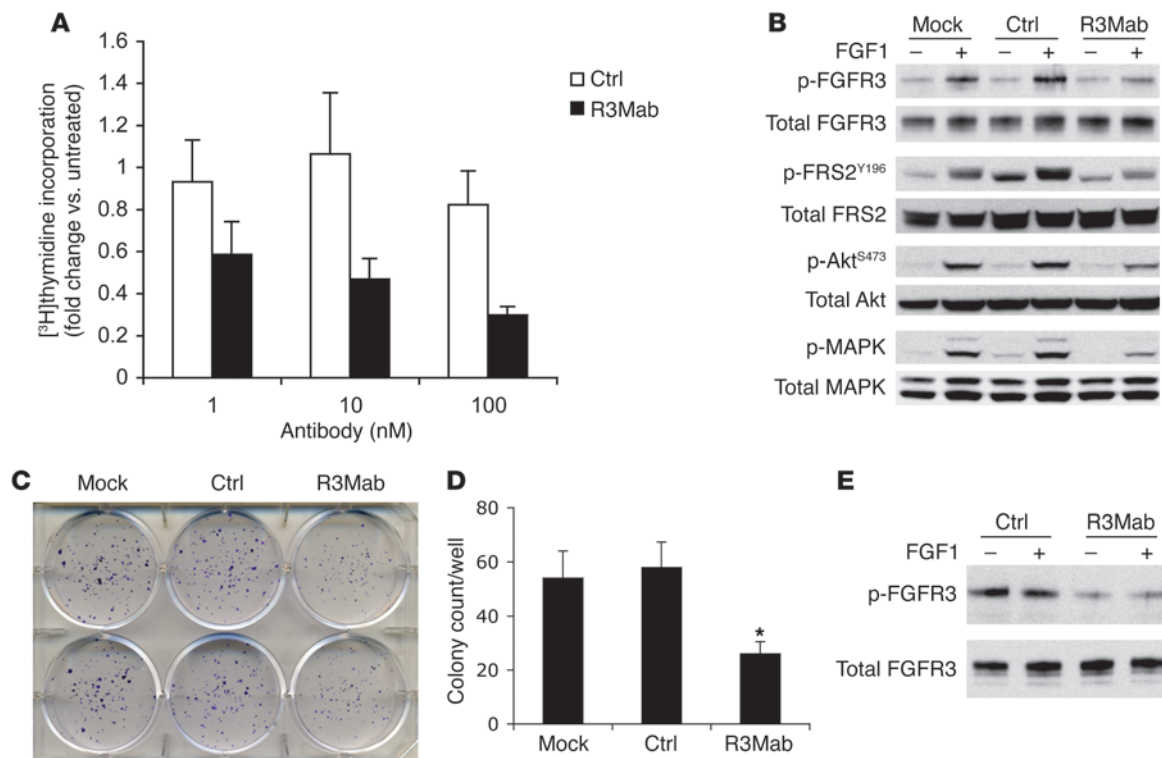
ed a significant, though more moderate suppression of RT4 cell proliferation (Supplemental Figure 5A). To investigate R3Mab's effect on FGFR3 activation, we examined the phosphorylation of FGFR3 in RT112 cells. Consistent with the results in Ba/F3-FGFR3 cells (Figure 3B), R3Mab markedly attenuated FGF1-induced FGFR3 phosphorylation (Figure 5B). We next examined phosphorylation of FRS2α, Akt, and p44/42 MAPK, three downstream mediators of FGFR3 signaling. FGF1 strongly activated these molecules in RT112 cells, while R3Mab significantly diminished this activation (Figure 5B). Similarly, R3Mab suppressed FGF1-induced phosphorylation of FGFR3 and MAPK in RT4 cells (Supplemental Figure 5B).

We next investigated whether R3Mab could inhibit activation of endogenous mutant FGFR3 in human bladder cancer cells. S249C is the most frequent FGFR3 mutation in bladder cancer (Figure 3C). Two available cell lines, UMUC-14 and TCC-97-7, carry a mutated FGFR3^{S249C} allele (ref. 36 and data not shown). Although R3Mab did not affect the exponential growth of UMUC-14 cells in

culture (data not shown), it significantly reduced the clonal growth of these cells (Figure 5C). Specifically, R3Mab decreased the number of colonies larger than 120 μm in diameter by approximately 55% as compared with control antibody (Figure 5D). Furthermore, R3Mab inhibited [³H]thymidine incorporation by TCC-97-7 cells in culture (Supplemental Figure 5C).

The S249C mutation is reported to result in ligand-independent activation of FGFR3 (26, 30). Indeed, FGFR3^{S249C} was constitutively phosphorylated irrespective of FGF1 treatment in UMUC-14 cells and TCC-97-7 cells, while R3Mab reduced constitutive phosphorylation of FGFR3^{S249C} as compared with control antibody in both cell lines (Figure 5E and Supplemental Figure 5D).

R3Mab inhibits dimer formation by FGFR3^{S249C}. The ability of R3Mab to inhibit constitutive FGFR3^{S249C} signaling and proliferation in bladder cancer cells was surprising, considering that this mutant can undergo disulfide-linked, ligand-independent dimerization (26, 30). To explore how R3Mab inhibits FGFR3^{S249C}, we examined the effect of R3Mab on the oligomeric
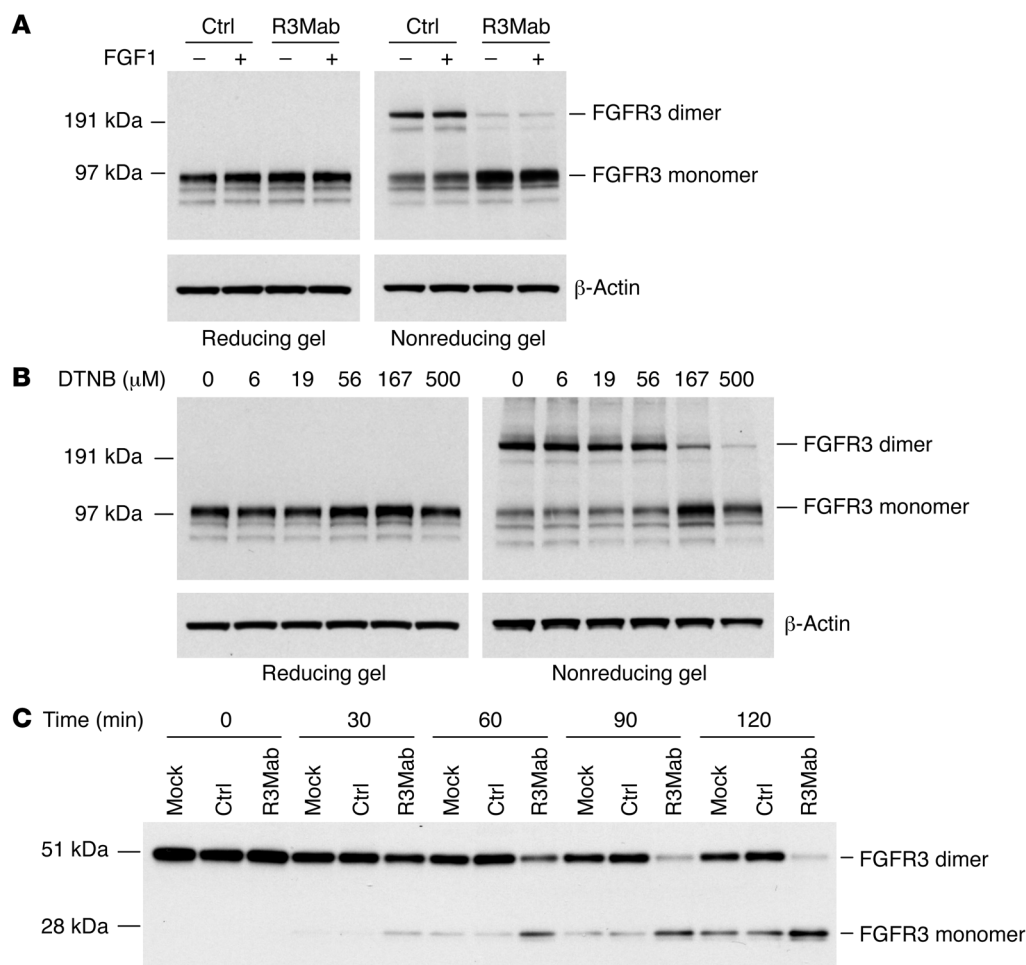
Figure 5
R3Mab inhibits proliferation, clonal growth, and FGFR3 signaling in bladder cancer cells expressing WT or mutated FGFR3^{S249C}. (**A**) Inhibition of [³H]thymidine incorporation by R3Mab in bladder cancer cell line RT112. Error bars represent SEM. (**B**) Blocking of FGF1-activated FGFR3 signaling by R3Mab (15 µg/ml) in bladder cancer cell line RT112 as compared with treatment medium alone (Mock) or a control antibody (Ctrl). Cell lysates were immunoprecipitated with anti-FGFR3 antibody and assessed for FGFR3 phosphorylation with an anti–phospho-tyrosine antibody (4G10). Lysates were immunoblotted to detect phosphorylation of Akt (p-Akt^{S473}) and p44/42 MAPK (p-MAPK$^{Thr202/Tyr204}$). (**C**) Inhibition of clonal growth by R3Mab (10 µg/ml) in bladder cancer cell line UMUC-14 (harboring FGFR3^{S249C}) as compared with treatment medium alone or a control antibody. (**D**) Quantitation of the study in **C** reporting the number of colonies larger than 120 µm in diameter per well from a replicate of 12 wells. Error bars represent SEM. *$P < 3.4 \times 10^{-9}$ versus Mock or Ctrl. (**E**) Inhibition of FGFR3 phosphorylation in UMUC-14 cells by R3Mab (15 µg/ml). FGFR3 phosphorylation was analyzed as in **B**. Note the constitutive phosphorylation of FGFR3 in this cell line.

state of this mutant in UMUC-14 cells. Under reducing conditions, FGFR3^{S249C} migrated as a single band of approximately 97 kDa, consistent with its monomeric size (Figure 6A). Under nonreducing conditions, in cells treated with control antibody, a large fraction of FGFR3^{S249C} appeared as a band of approximately 200 kDa, regardless of FGF1 addition, indicating a constitutive dimeric state (Figure 6A). R3Mab treatment substantially decreased the amount of dimers, with a concomitant increase in monomers (Figure 6A). Consistently, R3Mab decreased the level of FGFR3^{S249C} dimers in TCC-97-7 cells irrespective of FGF1 treatment (Supplemental Figure 5E).

How does R3Mab decrease the FGFR3^{S249C} dimer levels in bladder cancer cells? One potential explanation is that it may disrupt the FGFR3^{S249C} dimer through antibody-induced FGFR3 internalization and trafficking through endosomes or lysosomes. We tested this possibility by pharmacologically intervening with endocytosis. R3Mab nonetheless decreased the amount of dimer in UMUC-14 cells pretreated with various endocytosis inhibitors, despite substantial blockade of FGFR3^{S249C} internalization (Supplemental Figure 6, A and B). Thus, dimer disruption by R3Mab is independent of endocytosis. Another possible explanation is that cellular FGFR3^{S249C} may exist in a dynamic

monomer-dimer equilibrium; accordingly, binding of R3Mab to monomeric FGFR3^{S249C} could prevent dimer formation and thereby shift the equilibrium toward the monomeric state. To examine this possibility, we used the non-cell-permeating agent 5,5′-dithiobis 2-nitrobenzoic acid (DTNB), which selectively reacts with and blocks free sulfhydryl groups of unpaired cysteines (37). Treatment of UMUC-14 cells with DTNB led to the accumulation of FGFR3^{S249C} monomers at the expense of dimers (Figure 6B), indicating that FGFR3^{S249C} exists in a dynamic equilibrium between monomers and dimers.

To test whether R3Mab affects this equilibrium, we generated a soluble recombinant protein comprising the IgD2–D3 domains of FGFR3^{S249C} and isolated the dimers by size-exclusion chromatography. We incubated the dimers with buffer or antibodies in the presence of a very low concentration of reducing agent (25 µM DTT) and analyzed the oligomeric state of the receptor by SDS-PAGE under nonreducing conditions. R3Mab significantly accelerated the appearance of an approximately 25-kDa band representing monomeric FGFR3^{S249C} at the expense of the approximately 50-kDa dimer, as compared with mock or antibody controls (Figure 6C); indeed, by 2 hours the decrease in dimers was substantially more complete in the presence of

Figure 6
R3Mab decreases the steady-state level of disulfide-linked FGFR3^{S249C} dimer by driving the dimer-monomer equilibrium toward the monomeric state. (**A**) Effect of R3Mab on FGFR3^{S249C} dimer in UMUC-14 cells. Cells were incubated with R3Mab (15 μg/ml) or a control antibody for 3 hours, and whole-cell lysates were analyzed by immunoblot under nonreducing and reducing conditions. (**B**) Effect of free-sulfhydryl blocker DTNB on FGFR3^{S249C} dimer-monomer equilibrium in UMUC-14 cells. UMUC-14 cells were treated with increasing concentrations of DTNB for 3 hours, and cell lysates were analyzed as in **A**. (**C**) Effect of R3Mab on purified recombinant FGFR3^{S249C} dimer in vitro. FGFR3^{S249C} dimer composed of IgD2–D3 monomers was purified by size-exclusion chromatography and incubated with PBS (Mock), a control antibody, or R3Mab at 37°C. Samples were collected at the indicated times for immunoblot analysis under nonreducing conditions. FGFR3 dimer-monomer equilibrium was analyzed using anti-FGFR3 hybridoma antibody 6G1 (**A**–**C**).

R3Mab. These results indicate that R3Mab shifts the equilibrium between the monomeric and dimeric states of FGFR3^{S249C} in favor of the monomer.

R3Mab inhibits growth and FGFR3 signaling in multiple tumor models. Next, we examined the effect of R3Mab on the growth of bladder cancer cells in vivo. We injected *nu/nu* mice with RT112 cells (which express WT FGFR3), allowed tumors to grow to a mean volume of approximately 150 mm³, and dosed the animals twice weekly with vehicle or R3Mab. Compared with vehicle control at day 27, R3Mab treatment at 5 or 50 mg/kg suppressed tumor growth by about 41% or 73% respectively (Figure 7A). Analysis of tumor lysates collected 48 or 72 hours after treatment showed that R3Mab markedly decreased the level of phosphorylated FRS2α (Figure 7B). Intriguingly, total FRS2α protein levels were also lower in R3Mab-treated tumors, suggesting that FGFR3 inhibition may further lead to downregulation of FRS2α. R3Mab

also lowered the amount of phosphorylated MAPK in tumors, without affecting total MAPK levels (Figure 7B). Thus, R3Mab inhibits growth of RT112 tumor xenografts in conjunction with blocking signaling by WT FGFR3.

We next investigated the effect of R3Mab on growth of xenografts expressing mutant FGFR3. R3Mab treatment profoundly attenuated the progression of Ba/F3-FGFR3^{S249C} tumors (Figure 7C). Moreover, R3Mab significantly inhibited growth of UMUC-14 bladder carcinoma xenografts (Figure 7D). To evaluate whether R3Mab impacts FGFR3^{S249C} activation in vivo, we assessed the level of FGFR3^{S249C} dimer in tumor lysates collected 24 or 72 hours after treatment. Under nonreducing conditions, the amount of FGFR3^{S249C} dimer was substantially lower in R3Mab-treated tumors as compared with the control group, whereas total FGFR3^{S249C} levels, as judged by the amount detected under reducing conditions, showed little change (Figure 7E). This find-
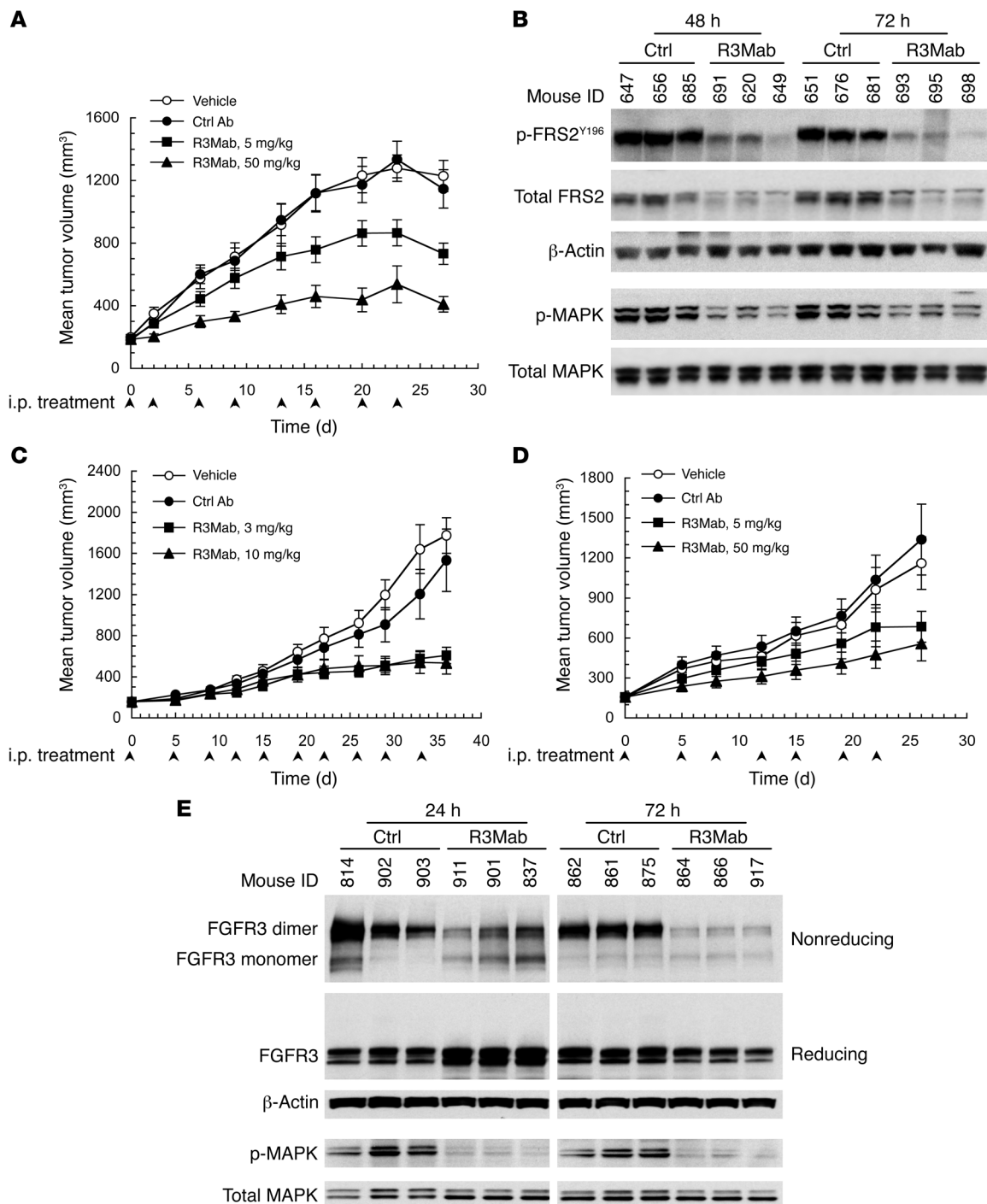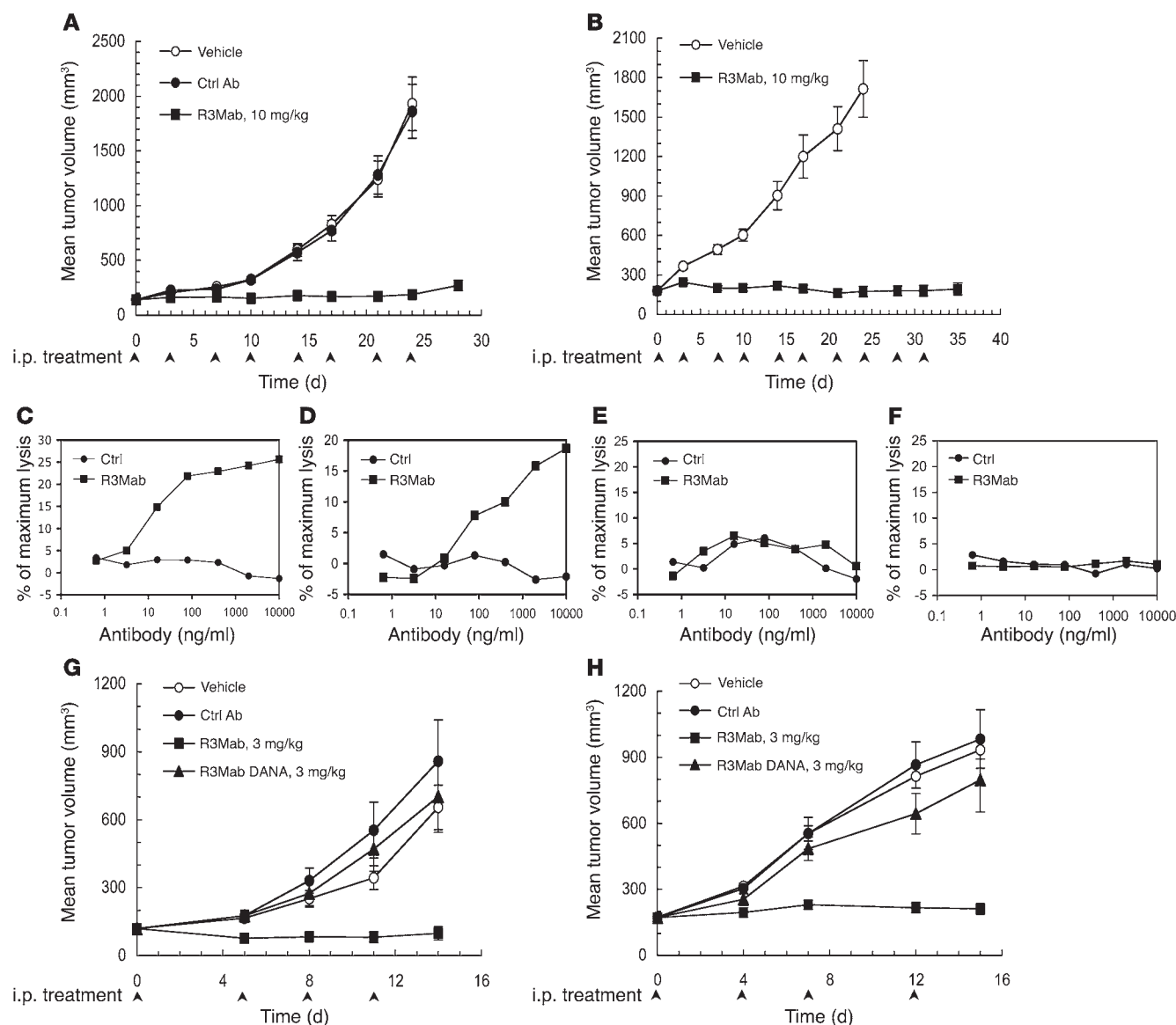
Figure 7
R3Mab inhibits xenograft growth of bladder cancer cells and allograft growth of Ba/F3-FGFR3[S249C]. (**A**) Effect of R3Mab on the growth of preestablished RT112 bladder cancer xenografts compared with vehicle control. $n = 10$ per group. (**B**) Inhibition of FGFR3 signaling in RT112 tumor tissues by R3Mab. In a separate experiment, RT112 xenograft tumors from mice treated with 15 mg/kg of a control antibody (Ctrl) or R3Mab for 48 or 72 hours were collected ($n = 3$ per group), homogenized, and analyzed for FRS2α and MAPK activation by immunoblot. (**C**) Effect of R3Mab on the growth of preestablished Ba/F3-FGFR3[S249C] allografts. $n = 10$ per group. (**D**) Effect of R3Mab on the growth of preestablished UMUC-14 bladder cancer xenografts. $n = 10$ per group. (**E**) Effect of R3Mab on FGFR3[S249C] dimer and signaling in UMUC-14 tumor tissues. UMUC-14 xenograft tumors from mice treated with 30 mg/kg of a control antibody or R3Mab for 24 or 72 hours were collected ($n = 3$ per group), homogenized, and analyzed for FGFR3[S249C] dimer-monomer equilibrium as well as MAPK activation by immunoblot. Note: FGFR3 dimer-monomer equilibrium was analyzed using anti-FGFR3 rabbit polyclonal antibody sc9007 to avoid interference from mouse IgG in tumor lysates. Error bars represent SEM.

Figure 8
ADCC contributes to the antitumor efficacy of R3Mab in t(4;14)-positive multiple myeloma models. (**A** and **B**) Effect of R3Mab on the growth of preestablished OPM2 (**A**) and KMS11 (**B**) myeloma xenografts. n = 10 per group. (**C**–**F**) Percent cytolysis of myeloma cell lines OPM2 (**C**) and KMS11 (**D**) or bladder cancer cell lines RT112 (**E**) and UMUC-14 (**F**) induced by R3Mab in cell culture. Myeloma or bladder cancer cells were incubated with freshly isolated human PBMCs in the presence of R3Mab or a control antibody. Cytotoxicity was determined by measuring lactate dehydrogenase (LDH) released in the supernatant. Maximum lysis was determined by incubation of the cells with detergent. (**G** and **H**) Effect of R3Mab or its DANA mutant on the growth of preestablished OPM2 (**G**) and KMS11 (**H**) myeloma xenografts. n = 10 per group. Error bars represent SEM and are sometimes smaller than symbols.

ing indicates that R3Mab inhibited dimerization of FGFR3[S249C] in vivo. No apparent accumulation of FGFR3[S249C] monomer was observed in tumor lysates, in contrast to the results in cell culture (compare Figure 7E and Figure 6A). This could be due to the weak detection sensitivity for monomeric FGFR3 under nonreducing conditions by the rabbit polyclonal anti-FGFR3 antibody used in this study (Supplemental Figure 7). Importantly, R3Mab also significantly inhibited the phosphorylation and activation of MAPK in UMUC-14 tumors (Figure 7E), suggesting that R3Mab inhibits the activity of FGFR3[S249C] in vivo. We did not observe any significant weight loss or other gross

abnormalities in any of the in vivo mouse studies. Furthermore, in a safety study conducted in mice, R3Mab, which binds with similar affinity to both human and murine FGFR3, did not cause any discernible toxicity in any organs, including bladder (data not shown). Together, these data indicate that multiple exposures to R3Mab are well tolerated in mice.

Antitumor activity of R3Mab in multiple myeloma xenograft models involves ADCC. To assess whether R3Mab might harbor therapeutic potential for multiple myeloma, we first tested the effect of R3Mab on the proliferation and survival of 3 t(4;14)-positive cell lines in culture. UTMC-2 cells carry WT FGFR3, while OPM2 and

KMS11 harbor K650E and Y373C substitutions, respectively (7). In culture, R3Mab completely abrogated FGF9-induced proliferation of UTMC-2 cells (Supplemental Figure 8A). R3Mab modestly inhibited the growth of OPM2 cells but had no apparent effect on the proliferation of KMS11 cells (Supplemental Figure 8, B and C). Since UTMC-2 cells do not form tumors in mice, we evaluated the efficacy of R3Mab against OPM2 and KMS11 tumors. R3Mab almost completely abolished xenograft tumor growth of both cell lines (Figure 8, A and B).

The marked difference in activity of R3Mab against OPM2 and KMS11 tumor cells in vitro and in vivo suggested the possibility that R3Mab may be capable of supporting Fc-mediated immune effector functions against these FGFR3-overexpressing tumors. Both cell lines express high levels of CD55 and CD59 (data not shown), 2 inhibitors of the complement pathway; accordingly, no complement-dependent cytotoxicity was observed (data not shown). We then focused on ADCC. ADCC occurs when an antibody binds to its antigen on a target cell and, via its Fc region, engages Fcγ receptors (FcγRs) expressed on immune effector cells (38). To test ADCC in vitro, we incubated KMS11 or OPM2 cells with freshly isolated human PBMCs in the presence of R3Mab or control antibody. R3Mab mediated substantial PBMC cytolytic activity against both myeloma cell lines (Figure 8, C and D). By contrast, R3Mab did not support cytolysis of bladder cancer RT112 or UMUC-14 cells (Figure 8, E and F). As measured by Scatchard analysis, the multiple myeloma cells expressed substantially more cell-surface FGFR3 than the bladder carcinoma cell lines (~5- to 6-fold more receptors per cell; Supplemental Figure 9, A and B).

To address the contribution of ADCC to the activity of R3Mab in vivo, we introduced the previously characterized D265A/N297A (DANA) mutation into the antibody's Fc domain. This dual substitution in the Fc domain of an antibody abolishes its binding to FcγRs (39), preventing recruitment of immune effector cells. The DANA mutation did not alter R3Mab binding to FGFR3 or inhibition of FGFR3 activity in vitro, nor did it change the pharmacokinetics of R3Mab in mice (data not shown); however, it substantially abolished in vivo activity against OPM2 or KMS11 xenografts (Figure 8, G and H). By contrast, the DANA mutation did not alter the antitumor activity of R3Mab toward RT112 and UMUC-14 bladder cancer xenografts (Supplemental Figure 10, A and B). Together, these results suggest that Fc-dependent ADCC plays an important role in the efficacy of R3Mab against OPM2 and KMS11 multiple myeloma xenografts.

Discussion

The association of FGFR3 overexpression with poor prognosis in t(4;14)-positive multiple myeloma patients and the transforming activity of activated FGFR3 in several experimental models have established FGFR3 as an important oncogenic driver and hence a potential therapeutic target in this hematologic malignancy. In contrast, despite reports of a high frequency of mutation and/or overexpression of FGFR3 in bladder carcinoma (24, 25, 40), a critical role for FGFR3 signaling in this epithelial malignancy has not been established in vivo. Moreover, the therapeutic potential of FGFR3 inhibition in bladder cancer has yet to be defined. Here we show that genetic or pharmacological intervention with FGFR3 inhibits growth of several human bladder cancer xenografts in mice. These results demonstrate that FGFR3 function is critical for tumor growth in this setting, underscoring the potential importance of this receptor as an oncogenic driver and therapeutic

target in bladder cancer. Blockade of FGFR3 function inhibited growth of xenografts expressing WT and mutant FGFR3 alike, suggesting that both forms of the receptor may contribute significantly to bladder tumor progression. Albeit much less frequently than in bladder cancer, FGFR3 mutations or overexpression have been identified in other solid tumor malignancies, including cervical carcinoma (40), hepatocellular carcinoma (41), and non–small cell lung cancer (42, 43), suggesting a potential contribution of FGFR3 to additional types of cancer.

The apparent involvement of FGFR3 in diverse malignancies makes this receptor an intriguing candidate for targeted therapy. While small molecule compounds that can inhibit FGFR3 kinase activity have been described (18–22, 44), the close homology of the kinase domains within the FGFR family has hampered the development of FGFR3-selective inhibitors. The lack of selectivity of the reported inhibitors makes it difficult to discern the relative contribution of FGFR3 to the biology of specific cancer types; further, it may carry safety liabilities, capping maximal dose levels and thus limiting optimal inhibition of FGFR3. Therefore, to achieve selective and specific targeting of FGFR3, we turned to an antibody-based strategy. We reasoned that an optimal therapeutic antibody should be capable of blocking not only the WT but also the prevailing cancer-linked mutants of FGFR3. Furthermore, given that dimerization of FGFR3 is critical for its activation, an antibody that not only blocks ligand binding but also interferes with receptor dimerization could be superior. Additional desirable properties would include the ability to support Fc-mediated effector function and the long serum half-life conferred by the natural framework of a full-length antibody. We focused our screening and engineering efforts on identifying an antibody molecule that combines all of these features, leading to the generation of R3Mab. Binding studies demonstrated the ability of R3Mab to compete with FGF ligands for interaction with both the IIIb and IIIc isoforms of FGFR3. Further experiments with transfected BaF/3 cell lines confirmed the remarkable ability of R3Mab to block both WT and prevalent cancer-associated FGFR3 mutants. In addition, R3Mab exerted marked antitumor activity in several xenograft models of bladder cancer expressing either WT FGFR3 or FGFR3[S249C], which is the most common mutant of the receptor in this disease. Pharmacodynamic studies suggested that the antitumor activity R3Mab in these models is based on inhibition of FGFR3 signaling, evident by diminished phosphorylation of its downstream mediators FRS2α and MAPK. These data further reinforce the conclusion that FGFR3 is required for bladder tumor progression, as demonstrated by our FGFR3 shRNA studies.

FGFR3 mutations in bladder cancer represent one of the most frequent oncogenic alterations of a protein kinase in solid tumor malignancies, reminiscent of the common mutation of B-Raf in melanoma (45). Most of the activating mutations in FGFR3 give rise to an unpaired cysteine, leading to ligand-independent receptor dimerization and to various degrees of constitutive activation. A previous study using a monovalent anti-FGFR3 Fab fragment indicated differential inhibitory activity against specific FGFR3 mutants (46); however, the molecular basis for this variable effect was not investigated. Compared with monovalent antibody fragments, bivalent antibodies have the capacity to induce the clustering of antigens and, in the case of receptor tyrosine kinases, may cause receptor oligomerization and activation. Despite its full-length and bivalent configuration, R3Mab

displayed universal inhibition of WT FGFR3 and of a wide spectrum of FGFR3 mutants, including variants that are ligand dependent (FGFR3^{G372C}, FGFR3^{Y375C}), constitutively active (FGFR3^{R248C}, FGFR3^{S249C}), or both (FGFR3^{K652E}). These results raise the question: How does R3Mab antagonize both WT and various FGFR3 mutants, including disulfide-linked variants?

Based on sequence alignment with FGFR1, the peptide epitope recognized by R3Mab overlaps with FGFR3 residues involved in binding to ligand and heparin, as well as receptor dimerization. This conclusion was confirmed by crystallographic studies of the complex between R3Mab and the extracellular regions of FGFR3. The X-ray structure revealed that the antibody binds to regions of IgD2 and IgD3 that are critical for ligand-receptor interaction as well as receptor-receptor contact. Thus, R3Mab may block WT FGFR3 both by competing for ligand binding and by preventing receptor dimerization. R3Mab may employ a similar mechanism to inhibit FGFR3^{K652E}, which has low constitutive activity but requires ligand for full activation. Furthermore, R3Mab binding changes the relative orientation of FGFR3 IgD3 with respect to IgD2. This finding raises the formal possibility that the antibody might also inhibit receptor activation by forcing a conformation that is not conducive to signal transduction — a notion that requires further study.

To gain better insight into how R3Mab blocks FGFR3 variants possessing an unpaired cysteine, we analyzed the most common mutant, FGFR3^{S249C}, in greater detail. Experiments with the free sulfhydryl blocker DTNB indicated a dynamic equilibrium between the monomeric and dimeric state of FGFR3^{S249C}. A similar equilibrium between oxidized and reduced states modulated by endogenous redox regulators has been reported for NMDA receptors (47). Incubation of bladder cancer cells expressing FGFR3^{S249C} with R3Mab led to a decline in the amount of receptor dimers and a concomitant increase in the level of monomers. Moreover, the purified IgD2–D3 fragment of FGFR3^{S249C} formed dimers in solution; when incubated with R3Mab, the dimers steadily disappeared, while monomeric FGFR3^{S249C} accumulated. Taken together with our structural data, these results suggest that R3Mab captures monomeric FGFR3^{S249C} and hinders its dimerization. Over time, R3Mab shifts the equilibrium toward the monomeric state, blocking constitutive receptor activity. This mechanism might also explain how R3Mab inhibits other cysteine mutants of FGFR3.

Another important finding of this study was the potent antitumor activity of R3Mab against the t(4;14)-positive multiple myeloma cell lines OPM2 and KMS11 in vivo. In contrast, R3Mab had modest to minimal impact on proliferation or survival of these cells in culture. OPM2 and KMS11 cells express relatively high cell-surface amounts of FGFR3 (5- to 6-fold higher than those of RT112 and UMUC-14 bladder carcinoma cells). These higher antigen densities may permit R3Mab to support efficient recruitment of FcγR-bearing immune effector cells and activation of ADCC. Indeed, in the presence of human PBMCs, R3Mab mediated cytolysis of OPM2 and KMS11 cells, but not RT112 or UMUC-14 bladder cancer cells. Moreover, the DANA mutant version of R3Mab, which is incapable of FcγR binding, had no effect on KMS11 or OPM2 growth in vivo but still suppressed growth of RT112 and UMUC-14 tumors similarly to R3Mab. Together, these data indicate that R3Mab has a dual mechanism of antitumor activity: (a) In cells expressing lower surface levels of WT or mutant FGFR3, it blocks ligand-dependent or constitutive signaling; and (b) in cells expressing relatively high surface FGFR3 levels, it induces ADCC.

Our results also raise some new questions. First, it is unknown why the bladder cancer cell lines tested in this study display variable sensitivity to R3Mab. Such a differential response, which is common for targeted therapy, may be a reflection of the distinct genetic makeup of individual tumors. Indeed, Her2-positive breast cancer cells show variable sensitivity to anti-Her2 antibody (48), as do various cancer cells in response to anti-EGFR antibody (49). In this context, development of additional in vivo models for bladder cancer with WT and mutant FGFR3 is urgently needed to assess sensitivity to anti-FGFR3 molecules in animals. Moreover, elucidation of predictive biomarkers may help identify patients who can optimally benefit from FGFR3-targeted therapy. Second, because R3Mab did not induce tumor regression in the models we examined, future studies should explore whether R3Mab can cooperate with established therapeutic agents.

In conclusion, our findings implicate both WT and mutant FGFR3 as important for bladder cancer growth, thus expanding the in vivo oncogenic involvement of this receptor from hematologic to epithelial malignancy. Furthermore, our results demonstrate that both WT and mutant FGFR3 can be effectively targeted in tumors with a full-length antibody that combines the ability to block ligand binding, receptor dimerization, and signaling, as well as to promote tumor cell lysis by ADCC. These results provide a strong rationale for investigating antibody-based, FGFR3-targeted therapies in malignancies associated with activation and/or overexpression of this receptor.

Methods

Cell lines and cell culture. The cell lines RT112 and RT4 were obtained from ATCC. Cell lines OPM2 and Ba/F3 were purchased from the German Collection of Microorganisms and Cell Cultures (DSMZ). Multiple myeloma cell line KMS11 was provided by Takemi Otsuki of Kawasaki Medical School (Kurashiki, Japan). UTMC-2 myeloma cell line (7) was obtained from Alan Solomon (University of Tennessee, Knoxville, Tennessee, USA) through a Material Transfer Agreement between the University of Tennessee and Genentech. Bladder cancer cell line TCC-97-7 was a gift from Margaret Knowles of St James's University Hospital (Leeds, United Kingdom). UMUC-14 cell line was provided by H.B. Grossman (formerly of University of Michigan, Ann Arbor, Michigan, USA, and currently at the University of Texas MD Anderson Cancer Center, Houston, Texas, USA) through a Material Transfer Agreement between the University of Michigan and Genentech. The cells were maintained with RPMI medium supplemented with 10% FBS (Sigma-Aldrich), 100 U/ml penicillin, 0.1 mg/ml streptomycin and L-glutamine under conditions of 5% CO$_2$ at 37°C. Cell proliferation assay, clonal growth assay, ADCC assay, and FACS assay were performed as described in Supplemental Methods.

Generation of RT112 FGFR3 shRNA and Ba/F3-FGFR3 stable cells. See Supplemental Methods for details.

Selecting phage antibodies specific for FGFR3. Human phage antibody libraries with synthetic diversities in the selected CDRs were used for panning. For details, see Supplemental Methods.

ELISA binding studies and antibody epitope mapping. See Supplemental Methods for details.

Immunoprecipitation and immunoblotting analyses. See Supplemental Methods for details.

Crystallization, structure determination, and refinement. See Supplemental Methods for details. Coordinates and structure factors were deposited in the Protein Data Bank with accession code 3GRW.

FGFR3^S249C dimerization studies. UMUC-14 cells were grown in cysteine-free medium and treated with R3Mab or DTNB for 3 hours, and cell lysates were subject to immunoblot analysis under reducing or nonreducing conditions. For in vitro dimerization studies, FGFR3-IIIb^{S249C} (residues 143–374) was cloned into pAcGP67A vector (BD Biosciences) and expressed in T.ni Pro cells (Expression Systems). The recombinant protein was purified through a Ni-NTA column (QIAGEN) followed by a Superdex S200 column (GE Healthcare Life Sciences). Dimeric FGFR3^{S249C} was eluted in 25 mM Tris (pH 7.5) and 300 mM NaCl. R3Mab (1 μM) was incubated with FGFR3^{S249C} dimer (0.1 μM) at 37°C under the following conditions: 100 mM KH_2PO_4 (pH 7.5), 25 μM DTT, 1 mM EDTA, and 0.75 mg/ml BSA. Aliquots of the reaction were taken at the indicated times points, and the reaction was stopped by adding sample buffer without β-mercaptoethanol. Dimer-monomer was analyzed by immunoblot.

Xenograft studies. All studies were approved by Genentech's Institutional Animal Care and Use Committee. Female *nu/nu* mice or CB17 SCID mice, 6–8 weeks of age, were purchased from Charles River Laboratories. Female athymic nude mice were obtained from the National Cancer Institute–Frederick Cancer Center. Mice were maintained under specific pathogen–free conditions. RT112 shRNA stable cells (7 × 10^6), RT112 (7 × 10^6), Ba/F3-FGFR3^{S249C} (5 × 10^6), OPM2 (15 × 10^6), or KMS11 cells (20 × 10^6) were implanted subcutaneously into the flank of mice in a volume of 0.2 ml in HBSS/Matrigel (1:1 v/v; BD Biosciences). UMUC-14 cells (5 × 10^6) were implanted without Matrigel. Tumors were measured twice weekly using a caliper, and tumor volume was calculated using the formula: $V = 0.5 \times a \times b^2$, where *a* and *b* are the length and width of the tumor, respectively. When the mean tumor volume reached 150–200 mm^3, mice were randomized into groups of 10 and were treated twice weekly with i.p injection of R3Mab (0.3–50 mg/kg) or a control human IgG1 diluted in HBSS. Control animals were given vehicle (HBSS) alone.

Statistics. Pooled data are expressed as mean ± SEM. Unpaired, 2-tailed Student's *t* tests were used for comparison between 2 groups. A *P* value less than 0.05 was considered statistically significant in all experiments.

Address correspondence to: Jing Qing or Avi Ashkenazi, Department of Molecular Oncology, Genentech Inc., 1 DNA Way, South San Francisco, California 94080, USA. Phone: (650) 467-8266; Fax: (650) 467-8195; E-mail: jqing@gene.com (J. Qing). Phone: (650) 225-1853; Fax: (650) 467-8195; E-mail: aa@gene.com (A. Ashkenazi).

1. Eswarakumar, V.P., Lax, I., and Schlessinger, J. 2005. Cellular signaling by fibroblast growth factor receptors. *Cytokine Growth Factor Rev.* **16**:139–149.
2. L'Hote, C.G., and Knowles, M.A. 2005. Cell responses to FGFR3 signalling: growth, differentiation and apoptosis. *Exp. Cell Res.* **304**:417–431.
3. Dailey, L., Ambrosetti, D., Mansukhani, A., and Basilico, C. 2005. Mechanisms underlying differential responses to FGF signaling. *Cytokine Growth Factor Rev.* **16**:233–247.
4. Mohammadi, M., Olsen, S.K., and Ibrahimi, O.A. 2005. Structural basis for fibroblast growth factor receptor activation. *Cytokine Growth Factor Rev.* **16**:107–137.
5. Grose, R., and Dickson, C. 2005. Fibroblast growth factor signaling in tumorigenesis. *Cytokine Growth Factor Rev.* **16**:179–186.
6. Chang, H., et al. 2005. Immunohistochemistry accurately predicts FGFR3 aberrant expression and t(4;14) in multiple myeloma. *Blood.* **106**:353–355.
7. Chesi, M., et al. 1997. Frequent translocation t(4;14)(p16.3;q32.3) in multiple myeloma is associated with increased expression and activating mutations of fibroblast growth factor receptor 3. *Nat. Genet.* **16**:260–264.
8. Fonseca, R., et al. 2003. Clinical and biologic implications of recurrent genomic aberrations in myeloma. *Blood.* **101**:4569–4575.
9. Moreau, P., et al. 2002. Recurrent 14q32 translocations determine the prognosis of multiple myeloma, especially in patients receiving intensive chemotherapy. *Blood.* **100**:1579–1583.
10. Pollett, J.B., Trudel, S., Stern, D., Li, Z.H., and Stewart, A.K. 2002. Overexpression of the myeloma-associated oncogene fibroblast growth factor receptor 3 confers dexamethasone resistance. *Blood.* **100**:3819–3821.
11. Bernard-Pierrot, I., et al. 2006. Oncogenic properties of the mutated forms of fibroblast growth factor receptor 3b. *Carcinogenesis.* **27**:740–747.
12. Agazie, Y.M., Movilla, N., Ischenko, I., and Hayman, M.J. 2003. The phosphotyrosine phosphatase SHP2

is a critical mediator of transformation induced by the oncogenic fibroblast growth factor receptor 3. *Oncogene.* **22**:6909–6918.
13. Ronchetti, D., et al. 2001. Deregulated FGFR3 mutants in multiple myeloma cell lines with t(4;14): comparative analysis of Y373C, K650E and the novel G384D mutations. *Oncogene* **20**:3553–3562.
14. Chesi, M., et al. 2001. Activated fibroblast growth factor receptor 3 is an oncogene that contributes to tumor progression in multiple myeloma. *Blood.* **97**:729–736.
15. Plowright, E.E., et al. 2000. Ectopic expression of fibroblast growth factor receptor 3 promotes myeloma cell proliferation and prevents apoptosis. *Blood.* **95**:992–998.
16. Chen, J., et al. 2005. Constitutively activated FGFR3 mutants signal through PLCgamma-dependent and -independent pathways for hematopoietic transformation. *Blood.* **106**:328–337.
17. Li, Z., et al. 2001. The myeloma-associated oncogene fibroblast growth factor receptor 3 is transforming in hematopoietic cells. *Blood.* **97**:2413–2419.
18. Trudel, S., et al. 2004. Inhibition of fibroblast growth factor receptor 3 induces differentiation and apoptosis in t(4;14) myeloma. *Blood.* **103**:3521–3528.
19. Trudel, S., et al. 2005. CHIR-258, a novel, multitargeted tyrosine kinase inhibitor for the potential treatment of t(4;14) multiple myeloma. *Blood.* **105**:2941–2948.
20. Chen, J., et al. 2005. FGFR3 as a therapeutic target of the small molecule inhibitor PKC412 in hematopoietic malignancies. *Oncogene.* **24**:8259–8267.
21. Paterson, J.L., et al. 2004. Preclinical studies of fibroblast growth factor receptor 3 as a therapeutic target in multiple myeloma. *Br. J. Haematol.* **124**:595–603.
22. Grand, E.K., Chase, A.J., Heath, C., Rahemtulla, A., and Cross, N.C. 2004. Targeting FGFR3 in multiple myeloma: inhibition of t(4;14)-positive cells by SU5402 and PD173074. *Leukemia.* **18**:962–966.

23. Gomez-Roman, J.J., et al. 2005. Fibroblast growth factor receptor 3 is overexpressed in urinary tract carcinomas and modulates the neoplastic cell growth. *Clin. Cancer Res.* **11**:459–465.
24. Tomlinson, D.C., Baldo, O., Harnden, P., and Knowles, M.A. 2007. FGFR3 protein expression and its relationship to mutation status and prognostic variables in bladder cancer. *J. Pathol.* **213**:91–98.
25. van Rhijn, B.W., Montironi, R., Zwarthoff, E.C., Jobsis, A.C., and van der Kwast, T.H. 2002. Frequent FGFR3 mutations in urothelial papilloma. *J. Pathol.* **198**:245–251.
26. Tomlinson, D.C., Hurst, C.D., and Knowles, M.A. 2007. Knockdown by shRNA identifies S249C mutant FGFR3 as a potential therapeutic target in bladder cancer. *Oncogene.* **26**:5889–5899.
27. Martinez-Torrecuadrada, J., et al. 2005. Targeting the extracellular domain of fibroblast growth factor receptor 3 with human single-chain Fv antibodies inhibits bladder carcinoma cell line proliferation. *Clin. Cancer Res.* **11**:6280–6290.
28. Martinez-Torrecuadrada, J.L., et al. 2008. Antitumor activity of fibroblast growth factor receptor 3-specific immunotoxins in a xenograft mouse model of bladder carcinoma is mediated by apoptosis. *Mol. Cancer Ther.* **7**:862–873.
29. Ornitz, D.M., and Leder, P. 1992. Ligand specificity and heparin dependence of fibroblast growth factor receptors 1 and 3. *J. Biol. Chem.* **267**:16305–16311.
30. d'Avis, P.Y., et al. 1998. Constitutive activation of fibroblast growth factor receptor 3 by mutations responsible for the lethal skeletal dysplasia thanatophoric dysplasia type I. *Cell Growth Differ.* **9**:71–78.
31. Adar, R., Monsonego-Ornan, E., David, P., and Yayon, A. 2002. Differential activation of cysteine-substitution mutants of fibroblast growth factor receptor 3 is determined by cysteine localization. *J. Bone Miner. Res.* **17**:860–868.
32. Knowles, M.A. 2008. Novel therapeutic targets in bladder cancer: mutation and expression of FGF receptors. *Future Oncol.* **4**:71–83.
33. Naski, M.C., Wang, Q., Xu, J., and Ornitz, D.M. 1996.

Graded activation of fibroblast growth factor receptor 3 by mutations causing achondroplasia and thanatophoric dysplasia. *Nat. Genet.* **13**:233–237.

34. Plotnikov, A.N., Schlessinger, J., Hubbard, S.R., and Mohammadi, M. 1999. Structural basis for FGF receptor dimerization and activation. *Cell.* **98**:641–650.

35. Olsen, S.K., et al. 2004. Insights into the molecular basis for fibroblast growth factor receptor auto-inhibition and ligand-binding promiscuity. *Proc. Natl. Acad. Sci. U. S. A.* **101**:935–940.

36. Jebar, A.H., et al. 2005. FGFR3 and Ras gene mutations are mutually exclusive genetic events in urothelial cell carcinoma. *Oncogene.* **24**:5218–5225.

37. Ellman, G.L. 1959. Tissue sulfhydryl groups. *Arch. Biochem. Biophys.* **82**:70–77.

38. Adams, G.P., and Weiner, L.M. 2005. Monoclonal antibody therapy of cancer. *Nat. Biotechnol.* **23**:1147–1157.

39. Gong, Q., et al. 2005. Importance of cellular microenvironment and circulatory dynamics in B cell immunotherapy. *J. Immunol.* **174**:817–826.

40. Cappellen, D., et al. 1999. Frequent activating mutations of FGFR3 in human bladder and cervix carcinomas. *Nat. Genet.* **23**:18–20.

41. Qiu, W.H., et al. 2005. Over-expression of fibroblast growth factor receptor 3 in human hepatocellular carcinoma. *World J. Gastroenterol.* **11**:5266–5272.

42. Cortese, R., Hartmann, O., Berlin, K., and Eckhardt, F. 2008. Correlative gene expression and DNA methylation profiling in lung development nominate new biomarkers in lung cancer. *Int. J. Biochem. Cell Biol.* **40**:1494–1508.

43. Woenckhaus, M., et al. 2006. Smoking and cancer-related gene expression in bronchial epithelium and non-small-cell lung cancers. *J. Pathol.* **210**:192–204.

44. Xin, X., et al. 2006. CHIR-258 is efficacious in a newly developed fibroblast growth factor receptor 3-expressing orthotopic multiple myeloma model in mice. *Clin. Cancer Res.* **12**:4908–4915.

45. Davies, H., et al. 2002. Mutations of the BRAF gene in human cancer. *Nature.* **417**:949–954.

46. Trudel, S., et al. 2006. The inhibitory anti-FGFR3 antibody, PRO-001, is cytotoxic to t(4;14) multiple myeloma cells. *Blood.* **107**:4039–4046.

47. Gozlan, H., and Ben-Ari, Y. 1995. NMDA receptor redox sites: are they targets for selective neuronal protection? *Trends Pharmacol. Sci.* **16**:368–374.

48. Hudziak, R.M., et al. 1989. p185HER2 monoclonal antibody has antiproliferative effects in vitro and sensitizes human breast tumor cells to tumor necrosis factor. *Mol. Cell. Biol.* **9**:1165–1172.

49. Masui, H., et al. 1984. Growth inhibition of human tumor cells in athymic mice by anti-epidermal growth factor receptor monoclonal antibodies. *Cancer Res.* **44**:1002–1007.